# Activation Parameters for Ligand Escape from Myoglobin Proteins at Room Temperature

**Mark D. Chatfield, Kevin N. Walda, and Douglas Magde***

*Contribution from the Department of Chemistry, University of California, San Diego, La Jolla, California 92093-0314.* *Received June 19, 1989*

**Abstract:** Laser flash photolysis studies of the temperature dependence of the rate of escape of oxygen, methyl isocyanide, and *tert*-butyl isocyanide from horse heart myoglobin (HHMb) and the rate of escape of oxygen from sperm whale myoglobin (SWMb) are presented for neutral pH and the temperature range: 5-40 °C. Enthalpies, entropies, and Gibb's free energies of activation for ligand escape are derived. The room-temperature entropies of activation are small in magnitude: -2.2 to +5 eu. The activation energies, $E_a$, are largest for the alkyl isocyanide ligands: +8.8 and +8.2 kcal/mol for escape of methyl and *tert*-butyl isocyanide, respectively. For $O_2$, the $E_a$ values are slightly smaller: +5.9 kcal/mol, $HHMbO_2$ in 0.1 M bis-tris/0.1 M NaCl buffer; +8.1 kcal/mol, $HHMbO_2$ in 0.1 M phosphate buffer; +7.4 kcal/mol, $SWMbO_2$ in 0.1 M bis-tris/0.1 M NaCl buffer; and +7.8 kcal/mol, $SWMbO_2$ in 0.1 M phosphate buffer. The Gibb's free energies fall into the range +6 to +7.5 kcal/mol, with the values for the four oxymyoglobin-buffer systems tightly grouped about 7.4 kcal/mol. Multiexponential nanosecond geminate rebinding of oxygen is resolved for all four oxymyoglobin-buffer systems at temperatures below 10 °C. For $HHMbO_2$ in 0.1 M bis-tris/0.1 M NaCl buffer, multiexponential rebinding is observed at temperatures up to 25 °C. Three five-state models are treated in simple numerical simulations of the room temperature multiexponential rebinding time course for $HHMbO_2$. The data cannot be fit to a sequential barrier model but can be fit to either of two other models. One incorporates ligand migration between the usual heme pocket and another adjoining pocket that traps the ligand for some time before permitting it to return and exit from the protein by way of the usual gate. The other considers two distinct escape routes through the protein.

Myoglobin proteins reversibly store oxygen in mammalian muscle tissue. Great progress has been made in their structural characterization,[1-8] and they have proved popular for mechanistic studies as well. In particular, many details of ligand binding have been unraveled in recent years by laser flash photolysis. The pioneering glassy matrix studies by Frauenfelder and co-workers established a multistate, sequential rebinding mechanism[9] in rigid, low-temperature media. Transient absorption[10-20] and transient Raman[21,22] spectroscopies probe geminate rebinding processes at room temperature on both picosecond and nanosecond time scales. Two picosecond processes have been distinguished. The faster process ($\tau$ = 2-2.5 ps for CO, $O_2$, and NO) has been attributed to a reaction of the dissociated ligand with an incompletely relaxed heme.[18] We do not include that possibility in the kinetic model considered here. Although we also observe such changes, a major portion, at least, of such features depends on the intensity of the photolysis laser; and the previous study neither treated the process as intensity dependent nor described how they separated any linear component from the nonlinear portion. In any case, any recombination to unrelaxed porphyrin is presumably not very pertinent to explaining ordinary, thermal reactions. There is also evidence for a slower reaction ($\tau$ = 6-40 ps) of the ligand with ground-state heme.[17] The heme iron atom and the unbound ligand are thought to be within van der Waal's distance of each other, comprising a contact geminate pair. After a few tens of picoseconds, the contact pair will have been disrupted (at room temperature), and the ligand will wander more or less freely throughout the heme "pocket", which, presumably, can itself relax on that time scale. Thereafter, the ligand either reforms the contact pair (from which it may rebind to the iron atom) or escapes into the solvent surrounding the protein. These last processes occur on a time scale of tens to hundreds of nanoseconds. At these longer nanosecond times, the iron binding site and the ligand together constitute a protein-separated geminate pair. Bimolecular recombination of free, solvated ligands with deoxymyoglobin proteins occurs on the millisecond time scale for ligand concentrations commonly studied.[17]

The above scenario is to be considered a working hypothesis, a pictorial description based on our recently proposed four-state kinetic model for the room-temperature rebinding of $O_2$, NO, and several alkyl isocyanides to myoglobin proteins:[17]

$$\mathrm{I} \underset{k_{-1}}{\overset{k_1}{\rightleftharpoons}} \mathrm{II} \underset{k_{-2}}{\overset{k_2}{\rightleftharpoons}} \mathrm{III} \underset{k_{-3}}{\overset{k_3}{\rightleftharpoons}} \mathrm{IV}$$

I, II, III and IV represent the ligated protein, the contact pair, the separated pair, and deoxymyoglobin with the ligand in the solvent shell. Four-state models have been proposed by others,[9,15] but the specific constraints on the time scales for fluid solutions at ambient conditions and the sharp distinction between the contact pair, supposed to exist for any iron porphyrin reacting with any ligand in any liquid solvent, and the protein-separated pair, unique to proteins, are novel in our treatment. Specifying those details makes our model subject to the criticism that it is not yet established; however, it is just those details that make the model

(1) Norvell, J. C.; Nunes, A. C.; Schoenborn, B. P. *Science* **1975**, *190*, 568.
(2) Heidner, E. J.; Ladner, R. C.; Perutz, M. F. *J. Mol. Biol.* **1976**, *104*, 707.
(3) Takano, T. J. *J. Mol. Biol.* **1977**, *110*, 537.
(4) Baldwin, J. M. *J. Mol. Biol.* **1980**, *136*, 103.
(5) Phillips, S. E. V. *J. Mol. Biol.* **1980**, *142*, 531.
(6) Hanson, J. C.; Schoenborn, B. P. *J. Mol. Biol.* **1981**, *153*, 117.
(7) Phillips, S. E. V.; Schoenborn, B. P. *Nature* **1981**, *292*, 81.
(8) Kuriyan, J.; Wilz, S.; Karplus, M.; Petsko, G. A. *J. Mol. Biol.* **1986**, *192*, 133.
(9) Austin, R. H.; Beeson, K. W.; Eisenstein, L.; Frauenfelder, H.; Gunsalus, I. C. *Biochemistry* **1975**, *114*, 5355.
(10) Shank, C. V.; Ippen, E. P.; Bersohn, R. *Science* **1976**, *193*, 50.
(11) Noe, L. J.; Eisert, W. G.; Rentzepis, P. M. *Proc. Natl. Acad. Sci. U.S.A.* **1978**, *75*, 573.
(12) Alpert, B.; El Moshni, S.; Lindqvist, L.; Tfibel, F. *Chem. Phys. Lett.* **1979**, *64*, 11.
(13) Duddell, D. A.; Morris, R. J.; Richards, J. T. *J. Chem. Soc., Chem. Commun.* **1979**, 75.
(14) Sommer, J. H.; Henry, E. R.; Hofrichter, J. *Biochemistry* **1985**, *24*, 7380.
(15) Gibson, Q. H.; Olson, J. S.; McKinnie, R. E.; Rohlfs, R. J. *J. Biol. Chem.* **1986**, *261*, 10228.
(16) Jongeward, K. A.; Marsters, J. C.; Mitchell, M. J.; Magde, D.; Sharma, V. S. *Biochim. Biophys. Res. Commun.* **1986**, *140*, 962.
(17) Jongeward, K. A.; Magde, D.; Taube, D. J.; Marsters, J. C.; Traylor, T. G.; Sharma, V. S. *J. Am. Chem. Soc.* **1988**, *110*, 380.
(18) Petrich, J. W.; Poyart, C.; Martin, J. L. *Biochemistry* **1988**, *27*, 4049.
(19) Rohlfs, R. J.; Olson, J. S.; Gibson, Q. H. *J. Biol. Chem.* **1988**, *263*, 1803.
(20) Petrich, J. W.; Martin, J. L. *Chem. Phys.* **1989**, *131*, 31.
(21) Findsen, E. W.; Friedman, J. M.; Ondrias, M. R.; Simon, S. R. *Science* **1985**, *229*, 661.
(22) Findsen, E. W.; Friedman, J. M.; Ondrias, M. R. *Biochemistry* **1988**, *27*, 8719.

0002-7863/90/1512-4680$02.50/0 

subject to rigorous testing. Testing the thermodynamic validity of our model, which postulates identifiable intermediates for the picosecond and nanosecond ligand rebinding to ground-state deoxymyoglobin, requires the determination of the room-temperature Arrhenius parameters for the geminate steps. The focus of this paper is on ligand escape from the heme pocket, process $k_3$. We report activation energies, enthalpies, and entropies for the escape of $O_2$, methyl isocyanide, and *tert*-butyl isocyanide from horse heart myoglobin (HHMb) and for the escape of $O_2$ from sperm whale (SWMb) myoglobin. The findings are partially, but not completely, in accord with theoretical predictions.[23,24] We also report multiexponential nanosecond rebinding kinetics for $O_2$ (but not the alkyl isocyanides) with both proteins under certain conditions (but not all conditions). We speculate on possible elaboration of the four-state model in directions considered previously by molecular dynamics simulations.[23]

## Experimental Procedures

Lyophilized sperm whale (type III) and horse heart (type III) myoglobin proteins were purchased from Sigma and used without further purification. Sodium dithionite, purchased from Virginia Chemical Corp., bis-tris (bis(2-hydroxyethyl)amine tris(hydroxymethyl)methane), purchased from Behring Diagnostics, and sodium phosphate (monobasic monohydrate and dibasic heptahydrate), purchased from Fischer Scientific, were used as received. Argon (Linde), oxygen (Linde), and *tert*-butyl isocyanide (Aldrich) were used as received. Methyl isocyanide was prepared from the corresponding formamide by literature procedures.[25] The alkyl isocyanide ligands and proteins were stored in the dark at 0 °C.

Aqueous buffers were prepared to give a 0.1 M bis-tris/0.1 M NaCl solution and a 0.1 M phosphate solution. The acidity was adjusted by the addition of small amounts of hydrochloric acid or sodium hydroxide to yield a pH of 7.0. The buffer solutions were stored at 5 °C and were used for 4 weeks after preparation. Solutions were deoxygenated by bubbling with argon.

The preparation of the oxymyoglobin and the alkyl isocyanide–myoglobin samples has been described previously.[17] In all of the samples, the concentration of the ligand was adjusted so that bimolecular rebinding was at least 10 times slower than geminate rebinding on the nanosecond time scale. All samples were diluted with buffer to give an absorbance of 1.2 at the Soret maximum in a 2-mm path length quartz sample cuvette. Static absorption spectra of the samples were recorded on a Varian DMS 300 UV–vis spectrophotometer before and after the experiments as a check for degradation.

Our nanosecond transient absorption spectrophotometer has been described in detail previously.[17] Briefly, an excimer-pumped dye laser provides photolysis pulses at 540 nm with a duration of 4 ns. The repetition rate is 1 Hz. Pulses from a xenon flashlamp pass through a 0.25-m monochromater and then probe the sample absorbance. The optical bandwidth is 5 nm. After the sample, the probe beam is filtered with glass filters and another small monochromater before striking the photomultiplier detector. The photocurrent is processed in a Biomation 6500 transient digitizer interfaced to a microcomputer. The Biomation is triggered by pulses from a photodiode monitoring the dye laser.

The sample cuvettes are mounted in a brass block thermostated to ±0.1 °C by a LAUDA RC3 water bath. The temperature is monitored by a calibrated chromel-alumel thermocouple potted to the brass block. The temperature dependence of the recombination kinetics are recorded by cycling from the low temperature (e.g., 5 °C) to the high temperature in 5 °C or 10 °C steps. The samples are allowed to equilibrate at each new temperature for 20 min before data are collected. Samples are exposed to pump and probe light only during data acquisition. For the alkyl isocyanide–myoglobin samples, 200 shots are averaged per run; for the oxymyoglobin samples, 500 shots. The Biomation time resolution is 2 ns per channel, and 1023 data points are recorded for each transient. For each transient recorded, a companion is recorded with the photolysing laser pulses blocked before the sample in order to account for subtle curvature in the base line. After converting the two transients to absorbance versus time files, the background trace is subtracted from the recombination time course. This corrected transient is used for curve-fitting rate analysis.

The extent of photolysis is limited to a small perturbation. The excitation pulse energy and spot size are adjusted so that MbCO, which has very little picosecond geminate recombination, exhibits about 20% dissociation. The parameters are maintained for other ligands, even though they do have picosecond recombination, which reduces the signals available on the nanosecond time scale. This avoids possible problems of absorption of multiple photons by an individual molecule or optical pumping of the same molecule through several dissociation–recombination cycles. It also explains the need for extensive signal averaging.

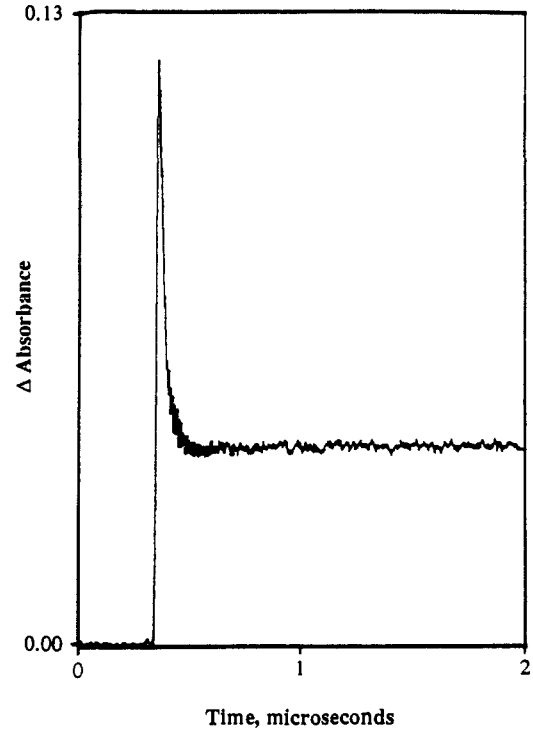


**Figure 1.** Transient absorption kinetics of HHMbCNMe in 0.1 M bis-tris, 0.1 M NaCl buffer, pH 7.0, 20 °C. The absorbance change at 440 nm is plotted versus delay time. Photolysis energy was 1 mJ at 540 nm.

## Results

**Escape of the Alkyl Isocyanides.** The nanosecond geminate rebinding of methyl and *tert*-butyl isocyanide (MeNC and *tert*-BuNC, respectively) to horse heart deoxymyoglobin is characterized by a single exponential decay over the temperature range 5–45 °C. A typical transient for HHMbCNMe in 0.1 M bis-tris/0.1 M NaCl buffer recorded at 20 °C is shown in Figure 1. Calculation of the rate of ligand escape from the heme pocket requires two parameters: the probability of escape, $\Gamma_{esc}$, and the observed rate constant, $k_{obs}$.[17] $\Gamma_{esc}$ is taken to be the ratio of the absorbance after 7 half-lives to the absorbance at the time of peak photolysis pulse power (see Figure 1). The instrument response to the photolysis pulse was monitored regularly and was characterized by a symmetrical peak with a reproducible FWHM of 11 ± 1 ns and a total duration of 36 ns. Because of electromagnetic interference from the excimer laser, formal deconvolution could not be justified. Consequently, the transient absorbance associated with the nanosecond processes was estimated by first truncating the records to include only absorbance readings occurring 36 ns or more after the onset of the photolysis pulse. The resulting files were fit to single exponentials by use of a Marquardt search for the least-squares fit.[26] The amplitudes of the best-fit curves were extrapolated 18 ns backward in time from the first point of the files to yield the absorbance at $t = 0$. (In our model, $\Gamma_{esc}$ should not be identified with the net, overall photodissociation yield $Q$. Rather, $Q$ is the product of $\Gamma$ factors that characterize each time scale separately. The clean separation of the picosecond and nanosecond time scales reported previously[17] justifies this procedure. Of course, it is possible that some limited amount of recombination occurs with characteristic time of a few nanoseconds, exactly in the domain most difficult to investigate. There is little reason to suspect such, except possibly for the case of $O_2$ as ligand, for reasons discussed earlier.[17]) The rate of ligand escape from the heme pocket is given by $k_3 = k_{obs} \times \Gamma_{esc}$.[17] Values for $k_{obs}$, $\Gamma_{esc}$, and $k_3$ for the HHMbCNMe and the HHMbCN*t*-Bu

(23) Case, D. A.; Karplus, M. *J. Mol. Biol.* **1979**, *132*, 343.
(24) Kottalam, J.; Case, D. A. *J. Am. Chem. Soc.* **1988**, *110*, 7690.
(25) Reisberg, P. I.; Olson, J. S. *J. Biol. Chem.* **1980**, *255*, 4144.

Table I. Parameters for Ligand Escape from Myoglobin

| protein/ligand | $T$, °C[a] | $k_{obs} \times 10^7$ s$^{-1}$ | $\Gamma_{esc}$ | $k_3 \times 10^7$ s$^{-1}$ |
|---|---|---|---|---|
| HNMbCNMe[b] | 5.4 | 2.37 ± 0.13 | 0.228 ± 0.008 | 0.541 ± 0.026 |
| HNMbCNMe[b] | 10.8 | 2.96 ± 0.05 | 0.239 ± 0.006 | 0.710 ± 0.024 |
| HNMbCNMe[b] | 15.4 | 3.42 ± 0.05 | 0.260 ± 0.006 | 0.890 ± 0.025 |
| HNMbCNMe[b] | 20.1 | 3.98 ± 0.09 | 0.308 ± 0.003 | 1.22 ± 0.02 |
| HNMbCNMe[b] | 25.2 | 4.62 ± 0.11 | 0.341 ± 0.011 | 1.58 ± 0.06 |
| HNMbCNMe[b] | 29.8 | 4.47 ± 0.09 | 0.419 ± 0.014 | 1.86 ± 0.11 |
| HNMbCNMe[b] | 34.3 | 5.00 ± 0.45 | 0.466 ± 0.010 | 2.32 ± 0.18 |
| HHMbCN*t*-Bu[b] | 5.4 | 1.20 ± 0.16 | 0.469 ± 0.272 | 0.560 ± 0.325 |
| HHMbCN*t*-Bu[b] | 20.5 | 1.88 ± 0.03 | 0.564 ± 0.050 | 1.06 ± 0.09 |
| HHMbCN*t*-Bu[b] | 30.1 | 2.59 ± 0.13 | 0.684 ± 0.049 | 1.77 ± 0.13 |
| HHMbCN*t*-Bu[b] | 39.7 | 3.30 ± 0.51 | 0.852 ± 0.12 | 2.80 ± 0.40 |
| $HHMbO_2$[b] | 6.3 | 0.572 ± 0.031 | 0.607 ± 0.013 | 0.347 ± 0.011 |
| $HHMbO_2$[b] | 15.9 | 0.862 ± 0.074 | 0.646 ± 0.009 | 0.556 ± 0.040 |
| $HHMbO_2$[b] | 25.4 | 1.14 ± 0.14 | 0.716 ± 0.009 | 0.818 ± 0.092 |
| $HHMbO_2$[b] | 34.9 | 1.18 ± 0.31 | 0.773 ± 0.030 | 0.908 ± 0.203 |
| $HHMbO_2$[c] | 6.3 | 0.505 ± 0.020 | 0.613 ± 0.003 | 0.309 ± 0.011 |
| $HHMbO_2$[c] | 15.9 | 0.693 ± 0.041 | 0.649 ± 0.003 | 0.450 ± 0.028 |
| $HHMbO_2$[c] | 25.4 | 0.947 ± 0.196 | 0.712 ± 0.007 | 0.674 ± 0.146 |
| $HHMbO_2$[c] | 34.9 | 1.50 ± 0.22 | 0.802 ± 0.014 | 1.22 ± 0.20 |
| $SWMbO_2$[b] | 6.3 | 0.504 ± 0.017 | 0.593 ± 0.001 | 0.299 ± 0.009 |
| $SWMbO_2$[b] | 15.9 | 0.788 ± 0.006 | 0.640 ± 0.005 | 0.505 ± 0.001 |
| $SWMbO_2$[b] | 25.4 | 1.05 ± 0.05 | 0.736 ± 0.002 | 0.771 ± 0.035 |
| $SWMbO_2$[b] | 34.9 | 1.28 ± 0.01 | 0.792 ± 0.043 | 1.01 ± 0.06 |
| $SWMbO_2$[c] | 6.3 | 0.531 ± 0.083 | 0.584 ± 0.009 | 0.310 ± 0.044 |
| $SWMbO_2$[c] | 15.9 | 0.752 ± 0.010 | 0.638 ± 0.008 | 0.480 ± 0.012 |
| $SWMbO_2$[c] | 25.4 | 0.972 ± 0.084 | 0.765 ± 0.032 | 0.744 ± 0.096 |
| $SWMbO_2$[c] | 34.9 | 1.47 ± 0.06 | 0.785 ± 0.031 | 1.15 ± 0.09 |

[a] Uncertainty = ±0.10 °C. [b] 0.1 M bis-tris/0.1 M NaCl buffer, pH 7.0. [c] 0.1 M phosphate buffer, pH 7.0.

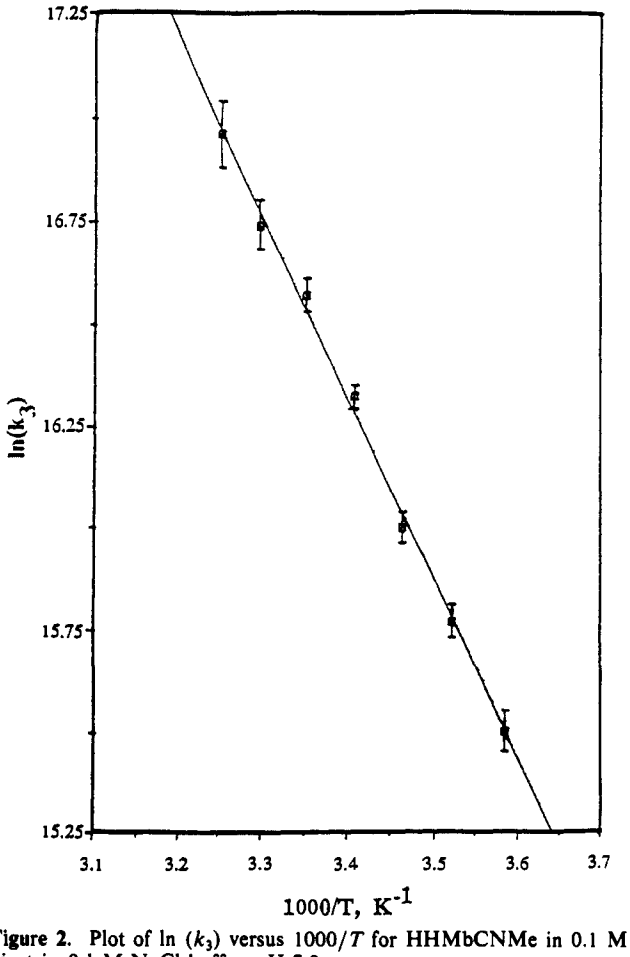


Figure 2. Plot of ln ($k_3$) versus $1000/T$ for HHMbCNMe in 0.1 M bis-tris, 0.1 M NaCl buffer, pH 7.0.

systems over the 5–45 °C temperature range are shown in Table I. Nanosecond geminate rates have not been reported previously for rebinding of alkyl isocyanide ligands to HHMb. Previous data have referred to the sperm whale analogue.[15,17] Comparison of the room-temperature rate and probability of escape of MeNC and *t*-BuNC from HHMb to corresponding values reported for

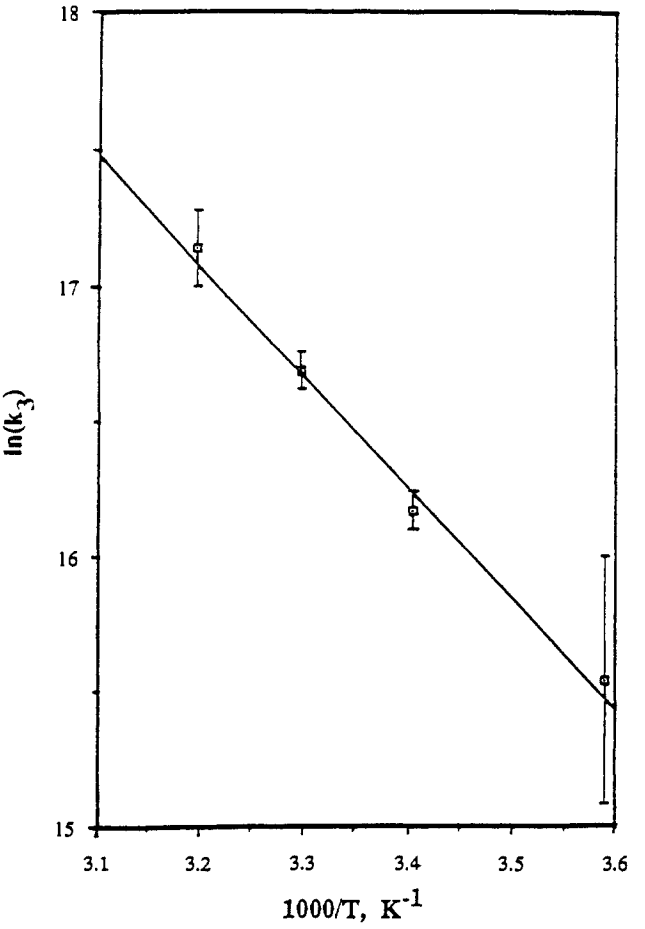


Figure 3. Plot of ln ($k_3$) versus $1000/T$ for HHMbCN*t*-Bu in 0.1 M bis-tris, 0.1 M NaCl buffer, pH 7.0.

Table II. Four-State Model Activation Parameters for Ligand Escape from Horse Heart and Sperm Whale Myoglobin

| protein/ligand | ln ($A$)[a] | $E_a$,[b] kcal/mol |
|---|---|---|
| HHMbCNMe[c] | 31.4 | 8.8 |
| HHMbCN*t*-Bu[c] | 29.9 | 8.2 |
| $HHMbO_2$[c] | 25.8 | 5.9 |
| $HHMbO_2$[d] | 29.4 | 8.1 |
| $SWMbO_2$[c] | 28.2 | 7.4 |
| $SWMbO_2$[d] | 29.1 | 7.8 |

[a] Uncertainty = ±0.75. [b] Uncertainty = ±1.0 kcal/mol. [c] 0.1 M bis-tris/0.1 M NaCl buffer, pH 7.0 [d] 0.1 M phosphate buffer, pH 7.0.

SWMb suggests that the magnitude of the protein-imposed barrier to escape of the alkyl isocyanides is greater in sperm whale myoglobin. Jongeward et al.[17] report rates and probabilities of escape of MeNC and *t*-BuNC from SWMb in 0.1 M bis-tris, NaCl buffer at pH 7.0, 20 °C: $k_3 = 5.9 \times 10^6$ s$^{-1}$ and $\Gamma_{esc} = 0.24 \pm 0.08$ for MeNC; and $k_3 = 3.6 \times 10^6$ s$^{-1}$ and $\Gamma_{esc} = 0.48 \pm 0.12$ for *t*-BuNC. These rates are roughly 50% smaller than our room temperature values for HHMb (see Table I). Gibson and Olson[15] report rates and probabilities for escape of the two alkyl isocyanide ligands from SWMb in 0.1 M phosphate buffer at pH 7.0 and room temperature: $k_3 = 4.9 \times 10^6$ s$^{-1}$ and $\Gamma_{esc} = 0.29$–$0.39$ for MeNC and $k_3 = 2.58 \times 10^7$ s$^{-1}$, and $\Gamma_{esc} = 0.63$ for *t*-BuNC. There is fairly good agreement between the two studies for SWMbCNMe, but a factor of six discrepancy between the two $k_3$ values reported for SWMbCN*t*-Bu.

Plots of ln ($k_3$) versus $1000/T$ for methyl and *tert*-butyl isocyanide rebinding are shown in Figures 2 and 3, respectively. Each point is the average of five separate measurements taken during an experiment, and the error bars indicate one standard deviation from the mean of the five measurements. The straight lines are linear least-squares fits to the equation

$$\ln (k_3) = \ln (A) - E_a/kT \quad (1)$$

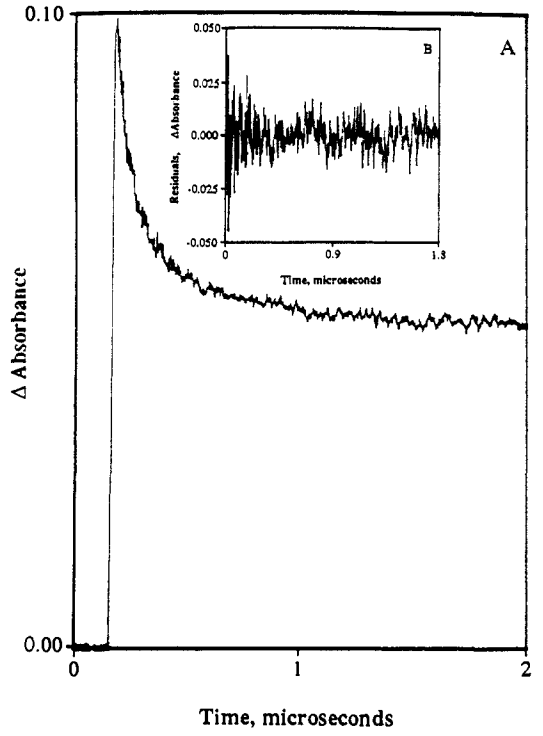


**Figure 4.** (a) Transient absorption kinetics of $HHMbO_2$ in 0.1 M bis-tris, 0.1 M NaCl buffer, pH 7.0, 6.3 °C. The absorbance change at 440 nm is plotted versus delay time. Photolysis energy was 2 mJ at 540 nm. (b) Residuals from the best biexponential fit to the transient in (a). Time zero is taken to be 18 ns after the onset of photolysis.

The fit is excellent. Frequency factors and activation energies are $4.2 \times 10^{13}$ $s^{-1}$ and 8.8 kcal/mol for HHMbCNMe and $1.0 \times 10^{13}$ $s^{-1}$ and 8.2 kcal/mol for HHMbCN*t*-Bu. These measurements were repeated three times, and the values for the Arrhenius parameters averaged over the three data sets are shown in Table II.

**Escape of Oxygen.** Nanosecond geminate rebinding of oxygen to HHMb and SWMb is more complex than the binding of alkyl isocyanide ligands. Below 10 °C, the rebinding time courses are multiexponential in both 0.1 M bis-tris/0.1 M NaCl buffer and 0.1 M phosphate buffer. A typical transient recorded for $HHMbO_2$ in bis-tris/NaCl buffer at 6.3 °C is shown in Figure 4A. Although there is no a priori justification for doing so, these rebinding time courses can be fit well to a sum of two exponentials. Figure 4B shows the residuals from the best biexponential fit to the time course in Figure 4A. The residuals exhibit a random distribution about a mean value of zero. Above 10 °C, the type of curvature exhibited in the rebinding time courses depends upon the combination of protein and buffer studied. At 15.9 °C and 25.4 °C, the rebinding of $O_2$ to horseheart myoglobin in bis-tris/NaCl buffer is biexponential in nature, whereas at 34.9 °C, the rebinding time courses are best fit to a single exponential. Table III contains the amplitude ratios and rates obtained from the biexponential fits. The indicated uncertainties are one standard deviation from the mean. The uncertainties in the amplitude ratios preclude trend analysis. The fitted rates show that the fast rate is 6 times larger than the slower rate at 6.3 °C, 15.9 °C, and 25.4 °C for the $HHMbO_2$/bis-tris/NaCl system, and the fast rate is 4 times larger than the slow rate at 6.3 °C for the three other protein/buffer systems studied. Multiexponential rebinding of ligands to myoglobin proteins has been reported previously. Gibson and Olson[15] studied nanosecond geminate rebinding of alkyl isocyanides to spermwhale myoglobin in 0.1 M phosphate buffer (pH 7.0, 20 °C). Biexponential fits to the rebinding time courses were required for *n*-propyl and *n*-butyl isocyanide but not for other alkyl isocyanides. Sommer et al.[14] also studied the nanosecond geminate rebinding of *n*-BuNC to SWMb, found that biexponential fits were required, and derived fitting parameters that were very similar, well within a factor of 2. Our fitting parameters

**Table III.** Biexponential Fitting Parameters for Nanosecond Geminate Rebinding of Oxygen to Horse Heart and Sperm Whale Myoglobin

| protein/ligand | $T$,[a] °C | $A_{g1}/A_{g2}$ | $k_{g1} \times 10^7$ $s^{-1}$ | $k_{g2} \times 10^6$ $s^{-1}$ |
|---|---|---|---|---|
| $HHMbO_2$[b] | 6.3 | 1.46 ± 0.48 | 1.71 ± 0.19 | 2.74 ± 0.55 |
| $HHMbO_2$[b] | 15.9 | 0.79 ± 0.16 | 3.67 ± 0.31 | 6.05 ± 0.94 |
| $HHMbO_2$[b] | 25.4 | 1.68 ± 0.07 | 3.37 ± 0.16 | 5.43 ± 0.58 |
| $HHMbO_2$[c] | 6.3 | 1.21 ± 0.51 | 1.14 ± 0.26 | 2.66 ± 0.33 |
| $SWMbO_2$[b] | 6.3 | 1.01 ± 0.31 | 1.31 ± 0.41 | 3.08 ± 0.46 |
| $SWMbO_2$[c] | 6.3 | 1.10 ± 0.47 | 1.03 ± 0.31 | 2.56 ± 0.09 |

[a] Uncertainty = ±0.10 °C. [b] 0.1 M bis-tris/0.1 M NaCl buffer, pH 7.0. [c] 0.1 M phosphate buffer, pH 7.0.

for the rebinding of $O_2$ to HHMb in bis-tris/NaCl buffer at 25.4 °C are similar: the fast rate lies between the values reported for the two *n*-alkyl isocyanides, while the slow rate is a little larger than either. The only conclusion we would draw from these similarities is that ligand behavior in the protein is not always sufficiently randomized to yield exponential kinetics. It does not seem likely that the detailed behavior of the three systems can be identical at the molecular dynamic level. There is some hint of multiexponential rebinding of $O_2$ to HHMb in phosphate buffer and to SWMb in both buffers at 15.9 °C; however, the amplitude ratios and rates derived from biexponential fitting were not reproducible. Often these time courses were just as well fit (as judged by a $\chi^2$ test) to single exponentials. At 25.4 °C and 34.9 °C, the rebinding of $O_2$ to HHMb in phosphate buffer and to SWMb in both buffers is cleanly single exponential in nature.

We also monitored the rebinding kinetics of $O_2$ to HHMb in bis-tris/NaCl buffer at 15.4 °C as a function of the probe wavelength. The amplitude ratios and rates derived from the biexponential fits for several wavelengths (430, 435, 440, and 445 nm) were the same within experimental uncertainty, indicating that the multiexponential nature of the time courses most probably does not arise as a consequence of spectral shifts induced by conformational relaxation of the protein, in agreement with recent nanosecond transient CD[27] and picosecond transient Raman studies[22] of protein conformational relaxation following photodetachment of CO from MbCO.

The multiexponential rebinding of oxygen suggests that our four-state model is an oversimplified description of the nanosecond geminate kinetics for $HHMbO_2$ and $SWMbO_2$, especially at temperatures below 10 °C. However, for purposes of comparison to our results for the alkyl isocyanide ligands, application of the four-state model analysis (as a first approximation) to our temperature dependence data does provide useful estimates of the Arrhenius parameters for escape of oxygen from the protein matrix. Single exponential fits to all of the rebinding time courses for the four oxymyoglobin-buffer systems yield the values for $\Gamma_{esc}$, $k_{obs}$, and $k_3$ shown in Table I. $\Gamma_{esc}$ is the most precisely determined parameter, and it shows little variation from one protein-buffer combination to the next at any particular temperature studied. Likewise, little variation is observed in $k_{obs}$ and $k_3$ among the four-oxymyoglobin-buffer systems at each temperature. Nanosecond geminate rates have not been reported previously for $HHMbO_2$. The results reported here for the rate and probability of escape of oxygen from SWMb in 0.1 M bis-tris/0.1 M NaCl buffer at pH 7.0 and 25.4 °C (Table I) are in reasonable agreement with our previously reported room-temperature values:[17] $k_3 = (8.8 \pm 1.6) \times 10^6$ $s^{-1}$ and $\Gamma_{esc} = 0.80 \pm 0.01$. The agreement is not quite as good, but still satisfactory, for other room-temperature photolysis studies. Gibson and Olson[15] report $k_3 = 1.44 \times 10^7$ $s^{-1}$ and $\Gamma_{esc} = 0.68$ for escape of $O_2$ from SWMb in 0.1 M phosphate buffer at pH 7.0 and room temperature. Duddel et al.[13] deduced a rate of $1.3 \times 10^7$ $s^{-1}$ for the escape of oxygen from sperm whale myoglobin. However an attempt to predict room-temperature values for the rate of escape of $O_2$ from SWMb in 0.1 M phosphate buffer (pH 7.0) from the low-temperature data of Frauenfelder et al.[9] yields $k_3 = 5 \times 10^5$ $s^{-1}$ (C → E transition in notation of ref 9). It is not really surprising that there could be a discrepancy between our room-temperature value ($k_3$

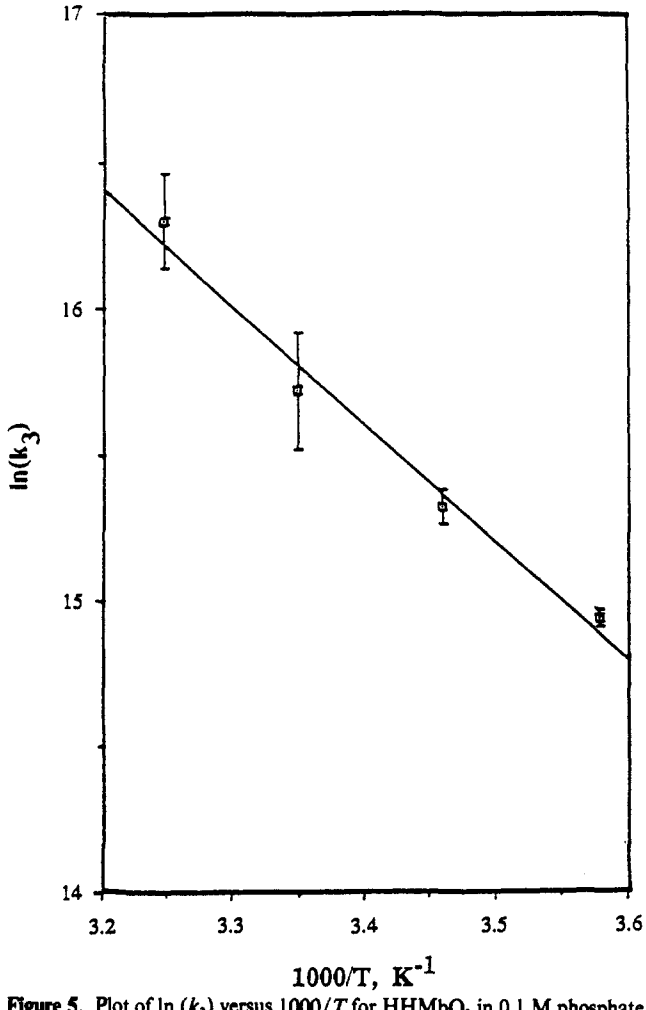


**Figure 5.** Plot of ln ($k_3$) versus $1000/T$ for $HHMbO_2$ in 0.1 M phosphate buffer, pH 7.0.

$= 7.44 \times 10^6\ s^{-1}$, Table I) and this extrapolation from a low-temperature, glycerol glass, but the precise manner in which low-temperature values differ from ambient is unclear. It has been suggested previously[24] that extrapolation of low-temperature kinetic parameters to room temperature may be unjustified.

A plot of ln ($k_3$) versus $1000/T$ for escape of oxygen from HHMb in phosphate buffer is shown in Figure 5. The best line-of-fit correlation coefficient is 0.99 for that phosphate data, The quality of straight line fits to plots for $HHMbO_2$ in bis-tris/NaCl buffer are not quite so good (typically $r = 0.96$–$0.98$). The correlation coefficients for $SWMbO_2$ in both buffers are typically 0.99–1.00. Values for ln ($A$) and the activation barrier heights derived from these fits are shown in Table II.

**Numerical Simulations of the Multiexponential Rebinding of Oxygen.** Once it became clear that under certain conditions of protein, ligand, buffer, and temperature kinetic traces were not the single exponentials we observed under other conditions, numerical integrations of several kinetic mechanisms were carried out in order to investigate what, if anything, might be concluded. The Gauss–Seidel iteration method[28] was employed in computer simulations of the nanosecond rebinding time course for $HHMbO_2$ in bis-tris/NaCl buffer at 25 °C. This time course was chosen because the picosecond rates for geminate recombination of $O_2$ to SWMb at 22 °C have been reported previously.[17] (The structure of the heme pocket is reportedly conserved between the metcyano derivatives of HHMb and SWMb in solution;[29] consequently we assume that picosecond geminate rebinding of $O_2$ to the two proteins occurs with similar rates. We have verified this experimentally, as will be discussed in a future publication.) Systems of coupled differential equations describing three five-state models were numerically integrated in 2 ps time increments for a total duration of 2 μs. The output files of the simulations described the total concentration of the deoxymyoglobin species at 2 ns intervals over the 2 μs duration of the simulation. Because the laser excitation pulse and the detection system response are both long compared to the characteristic times of the faster process described by the models, it is necessary to convolve the kinetic decays curves with the instrument response function. This is done simply by summing a distribution of kinetic decays calculated for δ function excitation weighted by the instrument response function. Such a treatment verifies that the details of the excitation and detection are not reflected in the more slowly decaying signals. Unfortunately, the use of an excimer laser generates an excess of electromagnetic interference that precludes any attempt to fit the detected signal in the first few nanoseconds.

**Scheme I**

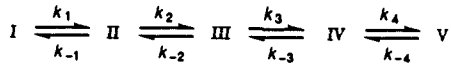


**Scheme II**

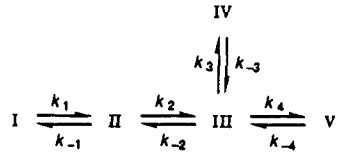


**Scheme III**

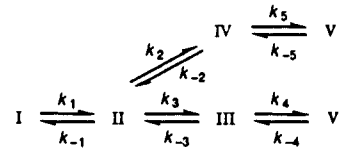


The three models considered were motivated by the molecular dynamics calculations of Case and Karplus[23] and can be described by the following kinetic schemes: In all of the schemes, I, II, III, and V represent the ligated protein, the contact pair, the separated pair (ligand in the heme pocket), and deoxymyoglobin with the ligand in the solvent shell, respectively. In Scheme I, IV could be pictured as a pocket outside of the heme pocket from which the ligand escapes to the solvent. State IV in Scheme II represents a second pocket adjoining the heme pocket into which a ligand may migrate and then return to the heme pocket. In Scheme III, IV represents an alternative separated pair from which the ligand escapes from the protein.

The initial concentrations of I, III, IV, and V were set to 0, while that of species II was set equal to 1. This is an arbitrary initial condition and not a statement about quantum yields; it reflects only our prior assertion that after the first few picoseconds of relaxation, ground-state five-coordinate contact pairs, species II, are already the photolysis product of six-coordinate hemes.[17] In the modeling of Schemes I and II, $k_1$ (the thermal off-rate), $k_{-1}$ (the contact pair rebinding rate), and $k_2$ (the rate of escape from the contact pair) were held constant (Table IV: $k_1$, $k_{-1}$, and $k_2$ are the same for Schemes I and II). The bimolecular recombination rates, $k_{-4}$ (Scheme I) and $k_{-3}$ (Scheme II), were set to zero because of the negligible contribution that bimolecular recombination makes during the 2-μs duration of the simulation. The remaining rate constants ($k_{-2}$, $k_3$, $k_{-3}$, and $k_4$ for Scheme I; $k_{-2}$, $k_3$, $k_4$, and $k_{-4}$ for Scheme II) were varied systematically to obtain the best match between the computed and measured amplitude ratio ($A_{g1}/A_{g2}$, Table III), observed nanosecond rates ($k_{g1}$ and $k_{g2}$, Table III), and probability of escape ($\Gamma_{esc}$, Table I) at 25.4 °C. Regardless of the choice of $k_{-2}$, $k_3$, $k_{-3}$, and $k_4$, Scheme I simulations did not yield a reasonable fit to the measured parameters. The observed rates could be reproduced very well, but

(26) Bevington, P. R. *Data Reduction and Error Analysis for the Physical Sciences*; McGraw-Hill: New York, 1969.
(27) Lewis, J. W.; Tilton, R. F.; Einterz, C. M.; Milder, S. J.; Kuntz, I. D.; Kliger, D. S. *J. Phys. Chem.* **1985**, *89*, 289.
(28) Kreyszig, E. *Advanced Engineering Mathematics*; John Wiley and Sons: New York, 1979.

**Table IV.** Fitted Rates from Five-State Model Numerical Simulations

| rate constant | Scheme II[a] | Scheme III[b] |
|---|---|---|
| $k_1$ $s^{-1}$ | 92 | 92 |
| $k_{-1} \times 10^{-10}$ $s^{-1}$ | 1.40 | 1.40 |
| $k_2 \times 10^{-10}$ $s^{-1}$ | 1.50 | 0.680 |
| $k_{-2} \times 10^{-7}$ $s^{-1}$ | 1.00 | 2.40 |
| $k_3 \times 10^{-7}$ $s^{-1}$ | 1.50 | 1.30 |
| $k_4 \times 10^{-9}$ $s^{-1}$ | 0.00570 | 8.20 |
| $k_{-4} \times 10^{-6}$ $s^{-1}$ | 5.40 | 1.00 |
| $k_5 \times 10^{-6}$ $s^{-1}$ | | 4.00 |

[a] $k_1$ taken from ref 15. $k_{-1}$ and $k_2$ taken from ref 17. [b] $k_1$ taken from ref 15. $k_{-1}$ taken from ref 17.

**Table V.** Numerical Simulation Curve-Fitting Parameters for Nanosecond Germinate Rebinding of Oxygen to Horse Heart Myoglobin[a]

| biexponential curve-fitting parameters | Scheme II | Scheme III | experimental[b] |
|---|---|---|---|
| $k_{g1} \times 10^{-7}$ $s^{-1}$ | 3.06 | 3.38 | 3.37 ± 0.16 |
| $k_{g2} \times 10^{-6}$ $s^{-1}$ | 5.48 | 5.46 | 5.43 ± 0.58 |
| $A_{g1}/A_{g2}$ | 1.64 | 1.67 | 1.68 ± 0.07 |
| $\Gamma_{esc}$ | 0.774 | 0.773 | 0.773 ± 0.032 |

[a] $HHMbO_2$, 0.1 M bis-tris/0.1 M NaCl buffer, pH 7.0, 25.4 °C. [b] $k_{g1}$, $k_{g2}$, and $A_{g1}/A_{g2}$ are from Table III, and $\Gamma_{esc}$ is from Table I.

the observed amplitude ratio and probability of escape could not be fit simultaneously. The requirement of a larger amplitude for the faster process ($A_{g1}/A_{g2}$ = 1.68) can only be met if the equilibrium between states III and IV is shifted toward state III. Conversely the constraint of a large probability of ligand escape from the protein ($\Gamma_{esc}$ = 0.77) requires that the equilibrium between III and IV be biased toward state IV, The sequential five-state model (Scheme I) cannot fit the observed time course.

Simulations with Scheme II were able to produce a more reasonable fit to the experimental parameters. Table IV contains the "best-fit" constants used in the simulations. The computed and experimental parameters are shown in Table V. The fit is not perfect, as evidenced by the slightly low computed value for the fast rate, $k_{g1}$. For the modelling of Scheme III, $k_1$ and $k_{-1}$ were fixed at constant values (Table IV). $k_{-3}$ and $k_{-5}$, the bimolecular recombination rates, were set to zero. $k_2$, $k_{-2}$, $k_3$, $k_4$, $k_{-4}$, and $k_5$ were varied in order to obtain the best fit to the experimental data. The sum of $k_2$ and $k_4$ was held fixed at the reported four-state model value for $k_2$ ($1.5 \times 10^{10}$ $s^{-1}$) for $SWMbO_2$ in bis-tris/NaCl buffer as a means of accounting for the observed picosecond rebinding parameters[17] for $SWMbO_2$. The "best-fit" rates are shown in Table IV. Table V contains the computed parameters. The match between the computed and experimental parameters is well within experimental error.

As a test of the ability of both Schemes II and III to account for the observed picosecond rebinding of oxygen to sperm whale myoglobin, numerical simulations of the picosecond rebinding were performed with the "best-fit" rates from Table V, covering a 1-ns interval in 2-ps steps. The initial concentrations of I, III, IV, and V were set equal to zero for both models. The initial concentration of II was 1.0. Both models predicted an observed picosecond rate and probability of escape from the contact pair of $3.0 \times 10^{10}$ $s^{-1}$ and 0.52, respectively. The reported values[17] are $(2.9 \pm 0.4) \times 10^{10}$ $s^{-1}$ and 0.52 ± 0.10.

## Discussion

It has been known for some time that the escape of a ligand from the heme pocket of myoglobin is an activated process. Neutron diffraction studies of the structure of oxymyoglobin reveal that paths leading from the distal coordination site of the heme iron atom to the exterior of the protein are blocked.[1] Frauenfelder et al. report sequential barriers 11 and 12 kcal/mol in magnitude to the escape of CO from MbCO in frozen glycerol/water.[9] Molecular dynamics calculations predict barriers to ligand escape whose amplitudes are modulated by cooperative displacements of key amino acid residues in the heme pocket region. Case and Karplus,[23] employing the rigid protein approximation, identified two likely escape paths. Along the simplest path, the ligand escapes the heme pocket by passing through a gate formed by the distal His E7 and Val E11 residues above the heme iron and then travels parallel to the heme plane in the direction of pyrrole IV to the solvent shell (Scheme I, Results section). The two computed sequential barriers along this path had activation energies of 6 and 13 kcal/mol. More recent calculations which allow for fluctuations of the protein environment during the migration of the ligand through the protein matrix predict that the barrier imposed by the His E7, Val E11 gate has $E_a$ approximately equal to 1 kcal/mol at room temperature.[24] The second escape path involves migration of the ligand through the B helix in the direction of the heme pyrrole II with a 17 kcal/mol energy barrier to escape imposed by the Leu B4 and Phe B14 protein residues. Also important in the context of our results is the identification of a second pocket above the heme plane separated from the heme pocket by a barrier due to the side chains of distal residues E11 and G8 (Scheme II, Results section). Case and Karplus noted that a significant number of ligand trajectories terminated in this second pocket during the 3.75-ps simulations and that diffusion of ligands between the two pockets might compete with ligand escape and thus modify the observed ligand rebinding time course.[23] Molecular dynamics simulations of binding and migration of xenon in metmyoglobin also predict ligand diffusion between pockets and multiple escape pathways.[30]

Our results confirm the presence of a sizable activation barrier to ligand escape from the heme pocket in room temperature aqueous solution. The activation energies given in Table II are quite similar (near 8 kcal/mol) for the three ligands, two species of myoglobin, and two buffers studied (with the exception of the $HHMbO_2$/bis-tris/NaCl system, for which $E_a$ is smaller). It is surprising that there is so little difference between oxygen and the alkyl isocyanides. In the rigid protein approximation the increased bulk of the isocyanides would be expected to give rise to a larger barrier to escape. The slightly larger activation energy for the escape of MeNC as compared to oxygen hints at this effect. On the other hand, the close correspondence between the activation energies for escape of *t*-BuNC and oxygen argues against the hypothesis. Our result can be rationalized by assuming that bulkier ligands distort the protein environment surrounding the heme cavity. Mims et al.[31] have suggested that incorporation of methyl isocyanide into the heme pocket must result in displacement of distal protein residues. This has been confirmed in a recent X-ray structure of the ethyl isocyanide complex of Mb.[32] If specific residues which obstruct the escape of the ligand are displaced from the positions occupied in oxymyoglobin, providing a wider gate through which the bulkier ligand can pass to the solvent shell, then the barrier to escape for the isocyanides need not be larger than that for $O_2$. An alternative hypothesis would be that the dominant escape pathways for $O_2$ and the bulkier alkyl isocyanide ligands are different, and it is coincidence that the activation barriers are nearly the same. We view the lower activation energy (5.9 kcal/mol, Table II) for escape of $O_2$ from HHMb in bis-tris/NaCl buffer as a convolution of barrier heights related to multiple paths. (See discussion of five-state model results below.)

It would be desirable to include the much-studied ligand CO in any discussion of activation energies. Unfortunately, CO shows very little geminate recombination to Mb at ambient conditions. The only data available refer to low-temperature, glycerol glasses.[9] For that system, the activation energy is 3–4 kcal/mol greater than for $O_2$ in ambient solution. It is reasonable that the barrier would be greater in glasses. Case and Kottalam computed the barrier to escape of $O_2$ from the heme pocket of sperm whale myoglobin to be 5 kcal/mol at 200 K, decreasing to 1 kcal/mol

(29) Lecomte, J. T. J.; La Mar, G. N. *Biochemistry* **1985**, *24*, 7388.
(30) Tilton, R. F., Jr.; Singh, U. C.; Weiner, S. J.; Connolly, M. L.; Kuntz, I. D., Jr.; Kollman, P. A.; Max, N.; Case, D. A. *J. Mol. Biol.* **1986**, *192*, 443.
(31) Mims, M. P.; Porras, A. G.; Olson, J. S.; Noble, R. W.; Peterson, J. A. *J. Biol. Chem.* **1983**, *258*, 14219.
(32) Johnson, K. A.; Olson, J. S.; Phillips, G. N., Jr., *J. Mol. Biol.* **1989**, *207*, 459.

Table VI. Thermodynamic Parameters for Ligand Escape from Horse Hearth and Sperm Whale Myoglobin

| protein/ligand | $\Delta S$,[a] eu | $\Delta H$,[b] kcal/mol | $\Delta G$[c] kcal/mol |
|---|---|---|---|
| HHMbCNMe,[d] $\kappa$ = 1.0 | +3.9 | +8.8 | +7.0 |
| HHMbCNMe,[d] $\kappa$ = 0.5 | +5.3 | +8.8 | +6.6 |
| HHMbCNMe,[d] $\kappa$ = 0.1 | +8.5 | +8.8 | +5.7 |
| HHMbCN*t*-Bu,[d] $\kappa$ = 1.0 | +1.7 | +8.2 | +7.3 |
| HHMbCN*t*-Bu,[d] $\kappa$ = 0.5 | +3.1 | +8.2 | +5.7 |
| HHMbCN*t*-Bu,[d] $\kappa$ = 0.1 | +6.3 | +8.2 | +6.7 |
| $HHMbO_2$[d] | −7.1 | +5.3 | +7.4 |
| $HHMbO_2$[e] | +0.1 | +7.5 | +7.5 |
| $SWMbO_2$[d] | −2.2 | +6.8 | +7.5 |
| $SWMbO_2$[e] | −0.5 | +7.2 | +7.3 |

[a] Uncertainty = ±1.5 eu. [b] Uncertainty = ±1.0 kcal/mol. [c] Uncertainty = ±1.1 kcal/mol. [d] 0.1 M bis-tris/0.1 M NaCl buffer, pH 7.0. [e] 0.1 M phosphate buffer, pH 7.0.

at 300 K.[24] However, the simulations do not take account of solvent, and Beece et al.[33] have noted that increasing the solvent viscosity (i.e., adding glycerol to water) slows the rate of ligand movement inside the protein in frozen solutions.

Examination of the entropies of activation reveals subtle differences between the pathways of escape of $O_2$ and the alkyl isocyanide ligands. According to transition-state theory, thermodynamic parameters are assigned to the activated complex following the prescription:[34]

$$\Delta H^{\ddagger} = E_a - RT \tag{2a}$$

$$\Delta G^{\ddagger} = -RT \ln [hk_3/\kappa kT] \tag{2b}$$

$$\Delta S^{\ddagger} = (\Delta H^{\ddagger} - \Delta G^{\ddagger})/T \tag{2c}$$

where the constants and variables are as follows: $\kappa$, the transmission coefficient; $k$, Boltzmann's constant; $T$, temperature; $h$, Planck's constant; $\Delta H^{\ddagger}$, $\Delta G^{\ddagger}$, and $\Delta S^{\ddagger}$, the activation enthalpy, Gibbs free energy, and entropy; and $R$, the universal gas constant. It may be important to note that besides the dependence on $T$ that is displayed explicitly, each of the thermodynamic parameters itself varies implicitly with temperature. This is not a cause for concern in comparing experimental data collected under comparable conditions, because the variations are expected to be small compared to other uncertainties. However, it should be kept in mind when making extrapolations of experimental data over large temperature ranges and in comparing experiment with molecular dynamics simulations. In their simulations, Case and Kottalam[24] estimate $\kappa$ = 0.91 for escape of $O_2$ from the heme pocket at 300 K. $\kappa$ was not estimated for escape of either of the alkyl isocyanide ligands. Three values of $\kappa$, 1.0, 0.5, and 0.1, suffice to cover the range of possibilities. The data of Table II were used to compute $\Delta S^{\ddagger}$ at 25 °C for the escape of $O_2$ from HHMb and SWMb in our four protein/buffer systems and the escape of the two isocyanides from HHMb. The results are shown in Table VI. The striking feature of these $\Delta S^{\ddagger}$ values is their small magnitudes. The magnitude of $\Delta S^{\ddagger}$ is buffer dependent for the oxymyoglobin samples. For $SWMbO_2$, $\Delta S^{\ddagger}$ is −2.2 eu in bis-tris/NaCl buffer and −0.5 eu in phosphate buffer. For $HHMbO_2$, $\Delta S^{\ddagger}$ is strongly buffer dependent; −7 eu in bis-tris/NaCl buffer and +0.1 eu in phosphate buffer. (The larger negative $\Delta S^{\ddagger}$ value for $HHMbO_2$ in bis-tris/NaCl buffer is a qualitative indicator at best due to the multiexponential nature of the rebinding at 25 °C.) The entropy of activation is positive for both isocyanide ligands: +3.9 eu ($\kappa$ = 1.0) for methyl isocyanide and +1.7 eu ($\kappa$ = 1.0) for *tert*-butyl isocyanide. Decreasing $\kappa$ increases the positive magnitudes of $\Delta S^{\ddagger}$ (Table VI), emphasizing an entropic difference between the escape of $O_2$ and the escape of the alkyl isocyanide ligands from myoglobin. The large uncertainties associated with $\Delta S^{\ddagger}$ values preclude a quantitative estimate of the difference. Previous estimates of $\Delta S^{\ddagger}$ for escape of $O_2$ from myoglobin are in disagreement with our values. Frauenfelder et al,[9] report a positive $\Delta S^{\ddagger}$ for the escape of $O_2$ from sperm whale myoglobin in 75/25 glycerol/water: +4.6 eu (C → E transition in the notation of ref 9). Since the reported error associated with this value is ±10%, the discrepancy cannot be attributed to poor precision in measurements. It more likely demonstrates that low-temperature values in glycerol solutions are not directly pertinent to physiological conditions.

Case and Kottalam[24] estimate the entropy of $O_2$ in the geminate state (in the heme pocket) at 20–25 eu, and they further suggest that much of this entropy is lost as oxygen passes through the His E7, Val E11 gate. If we accept the His E7, Val E11 gate as the major barrier to escape of O2 from the protein, then our data and model suggest that the rotational and translational degrees of freedom are less restricted than predicted as $O_2$ passes through the gate. Extending the "gated" escape model further to the alkyl isocyanide ligands, we would conclude that positive $\Delta S^{\ddagger}$ values are manifestations of a greater restriction on ligand mobility in the heme pocket than during passage of the ligand through the gate. Current experimental evidence is insufficient to allow us to further evaluate this point. However, the precision of our results seems sufficient to rule out entropy of activation as the major contributor to the barrier to escape of oxygen, MeNC, and *t*-BuNC from myoglobin.

The free energies of activation, $\Delta G^{\ddagger}$, at 25 °C for the escape of MeNC and *t*-BuNC from HHMb in bis-tris/NaCl buffer and the escape of $O_2$ from HHMb and SWMb in our four protein/buffer systems are also shown in Table VI. The $\Delta G^{\ddagger}$ values, like the activation energies, show little variation. Our results closely match the prediction of Case and Kottalam[24] of a free energy barrier of 7 kcal/mol for escape of oxygen from the heme pocket. While this close correspondence between empirically estimated and theoretically predicted $\Delta G^{\ddagger}$ values is intruiguing, their model predicts potential energy and entropic contributions of 1 and 6 kcal/mol, respectively, to $\Delta G^{\ddagger}$ at room temperature. Our data and model require a dominant potential energy contribution, 7.4–8.8 kcal/mol, and a small entropy contribution, 0 to −0.6 kcal/mol, to $\Delta G^{\ddagger}$. This represents a fundamental discrepancy, We had hoped to use a combination of the simulation plus our measurements to support the hypothesis that the (or, at least a) barrier to escape for oxygen is the distal His E7, Val E11 gate. As it is, we do not propose to abandon that hypothesis. The recent X-ray structure of Johnson et al.[32] offer added support for an already compelling case. Rather, we draw the conclusion that simulation and experiment are both improving in reliability but have not yet converged to a level of precision at which they can provide rigorous tests for each other.

The multiexponential rebinding of oxygen to horse heart and sperm whale myoglobin at pH 7.0 provides a greater challenge to mechanistic interpretation than the simple exponential rebinding usually observed on the nanosecond time scale. We must be cautious when interpreting nonexponential kinetics. The observations themselves are difficult. Only when the experimental procedure was improved and data averaging was increased to reduce relative noise, so as to be able to resolve small changes in rates at different temperatures, were we forced to confront nonexponential decays. The best argument that they are intrinsic and not instrumental artifact is that they are reproducible, albeit subtle, for particular sample conditions and not characteristic of all conditions. Even more important, one must be cautious when invoking models that produce biexponential kinetics. Once a single exponential is abandoned, innumerable functional forms and unlimited numbers of models become candidates that can fit the data equally well. Fitting parameters become highly correlated. Nevertheless, we believe that it is helpful to give some idea of what are the minimum modifications to previous kinetic models needed to fit our data within our confidence levels. Can previous schemes be "fixed up", or are we approaching the point at which we must abandon simple kinetic schemes altogether and depend on full molecular dynamic simulations?

(33) Beece, P.; Eisenstein, L.; Frauenfelder, H.; Good, D.; Marden, M. C.; Reinisch, L.; Reynolds, A. H.; Sorensen, L. B.; Yue, K. T. *Biochemistry* **1980**, *19*, 5147.

(34) Moore, J. W.; Pearson, R. G. *Kinetics and Mechanisms*; John Wiley and Sons: New York, 1981.

Our experimental results provide evidence for variations in rebinding mechanisms that depend upon the primary structure of the protein, the interaction of the protein with different buffers, and the temperature of the solution. The first effect is exemplified by the multiexponential rebinding of $O_2$ to HHMb and simple exponential rebinding of $O_2$ to SWMb in bis-tris/NaCl buffer at pH 7.0 and 25.4 °C. (The primary structures of horse heart and sperm whale myoglobin differ by virtue of 19 amino acid group substitutions.[35]) The importance of the protein-buffer interaction is well illustrated by the multiexponential rebinding of oxygen to HHMb in bis-tris/NaCl buffer and the simple exponential rebinding of $O_2$ to HHMb in phosphate buffer at pH 7.0 and 25.4 °C. The dependence of the rebinding mechanism upon solution temperature is demonstrated by the observation of multiexponential rebinding in only the $HHMbO_2$/bis-tris/NaCl system above 10 °C and in all four oxymyoglobin-buffer systems below 10 °C. In modelling the multiexponential rebinding at 25.4 °C, we sought mechanistic schemes which required the least parameterization beyond that already incorporated in the four-state model. The five-state sequential rebinding model (Schene I) is grossly inadequate, as we have already discussed. The five-state, two-pocket model (Scheme II) provides reasonable estimates of the four experimentally derived parameters (Table V), although the fast observed rate, $k_{g1}$, cannot be reproduced exactly without an accompanying overestimate of the other three parameters. The central prediction of this model is the modification of the nanosecond geminate rebinding of oxygen from the separated pair state by a near-equal partitioning of the ligands ($k_4/k_{-4} = 1.06$) between the heme pocket and an adjoining pocket in the distal protein domain. The observed fast nanosecond feature is described in this model as a competition among reformation of contact pairs from separated pairs, loss of ligands from the heme pocket to the adjoining pocket, and escape of ligands from the heme pocket to the solvent. The rate of the slower rebinding is controlled by the rate of return of ligands to the heme pocket from the adjoining pocket. In Scheme II, the predicted rate of escape of oxygen from the heme pocket of HHMb ($k_3 = 1.50 \times 10^7$ s$^{-1}$, Table IV) is very close to the values we report for escape of MeNC ($1.577 \times 10^7$ s$^{-1}$, Table I) and *t*-BuNC ($1.436 \times 10^7$ s$^{-1}$: computed with the activation parameters in Table II) at 25 °C, suggesting that the barriers to escape from HHMb are of the same magnitude for these ligands in bis-tris/NaCl buffer at pH 7.0. By contrast, the rates of escape of $O_2$ from HHMb in phosphate buffer and from SWMb in either buffer are roughly 50% smaller than $k_3$, implying that the barrier to escape is larger in these protein/buffer systems.

The five-state, parallel escape path model (Scheme III) provides the best fit to the experimental parameters and a radically different interpretation of the multiexponential rebinding of oxygen at room temperature. Nanosecond geminate rebinding and escape of oxygen occurs from two distinct separated pairs. Branching of the contact pair population into the two separated pair states (III and IV, Scheme III) occurs with approximately equal probability ($k_4/k_2 = 1.21$). The fast and slow observed rebinding are attributed to depopulation of states III and IV, respectively. The two derived rate constants for escape, $k_3 = 1.30 \times 10^7$ s$^{-1}$ and $k_5 = 4.00 \times 10^6$ s$^{-1}$, are respectively similar to the four-state model rates we report for the escape of the isocyanides from HHMb and for the escape of $O_2$ from HHMb (phosphate buffer, pH 7.0) and SWMb (bis-tris/NaCl and phosphate buffers). Thus the parallel escape path model suggests that the escape of MeNC and *t*-BuNC from HHMb in bis-tris/NaCl buffer may occur along a different path through the protein matrix as compared to escape of $O_2$ from HHMb in phosphate buffer and SWMb in both buffers.

We concur with Case and Kottalam[24] that further molecular dynamics studies of alternative escape routes are needed. Our results suggest that incorporation of protein-solvent and protein-buffer interactions will be required if accurate simulations of the energetics of escape are to be obtained. An explanation of the shift from multiexponential rebinding to exponential rebinding of oxygen to horse heart and sperm whale myoglobin in certain temperature ranges would be particularly useful. A simple interpretation is that as the temperature increases, the rates of passage of $O_2$ over activation barriers along different escape trajectories become roughly equal. Thus several competing escape processes would be indistinguishable from a single exponential rebinding time course in transient absorption studies.[36] Molecular dynamics simulations of the pathways and energetics of the escape of isocyanide ligands from myoglobin could also be of help in the identification of molecular properties that cause subtle differences in the energetics of the escape of these ligands as compared to oxygen. In the experimental vein, we need values for the picosecond geminate rates at temperatures other than 25 °C. Also valuable will be studies of the energetics of ligand escape as a function of site mutations in the primary structure of the protein (e.g., temperature dependence studies of the rate of escape of oxygen from cloned sperm whale myoglobin lacking the distal His E7 residue). Dramatic changes in the bimolecular association rates for alkyl isocyanide ligands and in the dissociation rate for $O_2$ with cloned sperm whale myoglobin proteins in which the distal histidine has been replaced with other amino acid groups have been reported.[37,38]

**Acknowledgment.** This research was supported in part by National Institutes of Health Grants 786220-24152 and RR02353-1 and National Science Foundation Grant CHE 8715561. We thank Professor T. G. Traylor of the University of California at San Diego for the methyl isocyanide used in this study. We thank Prof. J. S. Olson of Rice University and Dr. D. J. Taube and Dr. V. S. Sharma of the University of California at San Diego for many helpful suggestions and informative discussions.

(35) Puett, D. *J. Biol. Chem.* **1973**, *248*, 4623.

(36) A similar explanation was put forward by Austin and Frauenfelder (ref 9) in their interpretation of the temperature dependence of oxygen and carbon monoxide rebinding to sperm whale myoglobin in 75/25 glycerol/water.

(37) Springer, B. A.; Egeberg, K. D.; Sligar, S. G.; Rohlfs, R. J.; Mathews, A. J.; Olson, J. S. *J. Biol. Chem.* **1989**, *264*, 3057.

(38) Olson, J. S.; Mathews, A. J.; Rohlfs, R. J.; Springer, B. A.; Egeberg, K. D.; Sligar, S. G.; Tame, J.; Renaud, J. P.; Nagai, K. *Nature* **1988**, *336*, 265.